American Mineralogist, Volume 62, pages 286–295, 1977

Effects of temperature and pressure on the crystal structure of ferromagnesian olivine

ROBERT M. HAZEN[1]

Department of Geological Sciences, Harvard University
Cambridge, Massachusetts 02138

Abstract

Crystal structures of fayalite at −196° and 23°C, and at pressures of 31 and 42 kbar, have been refined from three-dimensional X-ray diffraction data. Fayalite component polyhedra respond to temperature and pressure in a manner similar to that of forsterite: octahedra possess thermal expansivities and compressibilities comparable to those of bulk fayalite, whereas SiO_4 tetrahedra vary little with changes in temperature and pressure. In fayalite, all Fe–O bonds expand at similar rates, unlike forsterite in which short Mg–O bond distances vary significantly less with temperature and pressure than long bonds.

Crystal-structure dimensions of forsterite, intermediate Mg–Fe olivine, and fayalite projected to their respective melting points are identical. Shared-edge misfit between expanding octahedra and rigid tetrahedra may account, in part, for olivine instability at its melting point. Mantle olivine from a depth of 100 km is predicted to have a structure which is similar to that of forsterite at 1 atm and 600°C. An equation of state for ferromagnesian olivines is:

$$V = (290 + 0.17X_{Fe} + 0.006T + 0.000006T^2)[1 - P/(1350 - 0.16T)]\ A^3,$$

where V is the unit-cell volume, X_{Fe} the octahedral mole fraction of iron, T the temperature in °C, and P the pressure in kbar.

Introduction

A previous study (Hazen, 1976a) presented information on the variation of the crystal structure of magnesian olivine (forsterite) with temperature and pressure. This report gives similar data, including atomic coordinates and thermal vibration parameters, for the ferrous iron olivine, fayalite. The principal objective of this study is to define systematic variations in the crystal structure of ferromagnesian olivines with changes in temperature, pressure, and Fe/Mg ratio. These systematic variations will then be used to predict the structure and stability of olivine as a function of temperature, pressure, and composition.

Experimental

Specimen description

Dr. T. Usselman (Smyth and Usselman, 1974) has synthesized crystals of fayalite (Fe_2SiO_4), and has kindly provided specimens of this material for study. Indices of refraction in white light are $\alpha = 1.828$, $\beta = 1.869$, and $\gamma = 1.880$ (all ± 0.002), which agree with those determined by Heinriques (1957). Crystals are transparent with a brownish-green color, and are optically free of fractures. An irregular crystal 200 × 250 × 250 μm was selected, mounted, and examined by X-ray photography. Fayalite was confirmed to have diffraction symmetry consistent with space group *Pbnm*.

Data collection at 23° and −196°C

Procedures for data collection from single crystals at room temperature and liquid-nitrogen temperature are as described by Hazen (1976b). Cell dimensions determined from four-circle diffractometer orientation data are given in Table 1. An independent determination by Smyth (1975) gave nearly identical results. 1137 symmetrically independent diffraction intensities were measured at room temperature (23°C), and these data were corrected for absorption effects using a linear absorption coefficient of 99.2

[1] Present address: Geophysical Laboratory, 2801 Upton Street, N.W., Washington, D.C. 20008.

TABLE 1. Olivine structure parameters and refinement conditions

T (°C)	P	Conditions	a(Å)	b(Å)	c(Å)	Vol(Å^3)	wR(%)	R(%)	No. of Measurements	No. of Observed	No. of Rejected*
Fayalite											
23	1 atm	Standard mount	4.818(2)†	10.470(4)	6.086(2)	307.0(3)	4.9	8.3	1137	571	0
-196	"	Cryo-Tip	4.814(2)	10.448(3)	6.076(2)	305.6(3)	5.6	5.7	678	570	20
23	"	In pressure cell	4.818(1)	10.473(5)	6.086(2)	307.1(3)	5.9‡	8.7‡	599	272	8
23	42 kb	"	4.801(4)	10.22(1)	6.049(6)	296.8(4)	7.0‡	10.9‡	965	258	26
23	31 kb	"	4.802(8)	10.26(3)	6.070(10)	299.1(10)	5.6‡	10.5‡	979	286	40
Hortonolite (Data of Smyth and Hazen, 1973), revised.											
23	1 atm	Evacuated silica capillary	4.798(5)	10.39(1)	6.055(6)	301.8(5)	3.1	5.1	1111	903	15
300	"	"	4.809(5)	10.42(1)	6.080(6)	304.6(5)	3.3	5.7	677	527	11
600	"	"	4.822(5)	10.46(1)	6.101(6)	307.6(5)	3.0	5.7	681	516	9
900	"	"	4.838(5)	10.49(1)	6.136(6)	311.5(5)	4.2‡	13.7‡	174	100	0

* $||F_{obs}| - |F_{calc}|| \geq 3.0$

† Parenthesized figures refer to the esd of least units cited.

‡ Isotropic temperature factors only.

cm^{-1}, for Mo$K\alpha$ radiation. The transmission varied from 36 to 62 percent, and 568 reflections were observed ($I > 2\sigma$); all space-group extinct reflections were absent. Convergence of the least-squares refinement was achieved at a weighted R = 4.9 percent, though the unweighted R was 8.3 percent, probably due to the lack of extinction correction. Refinement conditions are recorded in Table 1, and atom parameters and anisotropic temperature factors are listed in Tables 2 and 3 respectively. A similar refinement on the same material was completed by Smyth (1975), who kindly provided his prepublished data; Smyth's parameters of fayalite at 23°C are in close agreement with those of this study.

The fayalite crystal was remounted on a copper pin, and unit-cell and atomic parameters were determined at liquid-nitrogen temperature. Additional data on fayalite cell parameters from 300° to 900°C have been provided by Smyth (1975). Previously published preliminary data on the high-temperature crystal structures of a manganoan hortonolite from Franklin, New Jersey (Smyth and Hazen, 1973; composition $Mg_{0.75}Fe_{1.10}Mn_{0.15}SiO_4$) are here presented in revised form.

Data collection at 31 and 42 kbar

High-pressure X-ray diffraction techniques are similar to those of Hazen and Burnham (1974, 1975). High-pressure diffraction data have been corrected for diamond pressure-cell absorption as well as specimen absorption (Hazen, 1975b).

A fayalite crystal plate with good (010) cleavage, approximately 250 × 200 × 80 μm, was selected for preliminary high-pressure study. Since the high X-ray absorption by both the fayalite and the diamond pressure cell might introduce severe errors in observed structure factors, a reference refinement was made from room-pressure data measured on this crystal mounted within the diamond cell to test the effectiveness of our absorption correction procedures. Unit-cell parameters at 23°C and 1 atm were measured and agreed well with previous determinations. The average difference between the 11 refined positional variables of the two room T and P refinements is 0.004 fractional units.

Unfortunately this crystal was crushed as the diamond cell was tightened, and a second thin rectangular plate 240 × 180 × 40 μm was mounted, room-pressure cell parameters were confirmed, and the pressure cell was tightened again. Cell dimensions of a = 4.801 ± 0.004, b = 10.22 ± 0.01 and c = 6.049 ± 0.006 A were measured, giving a volume compression of 3.3 percent. Compression studies on olivine by Adams (1931) and Olinger and Halleck (1974) indicate the pressure of data collection to be approximately 42 ± 4 kbar. Only 258 of 965 nonequivalent reflections were observed, and transmission factors varied from 14 to 36 percent. These data converged to a weighted R of 7.0 percent (unweighted 10.9%). As in forsterite high-pressure data collection (Hazen, 1976a), low peak-to-noise ratios resulted in many unobserved reflections, as well as low precision for the observed reflections.

Due to peak broadening and consequent loss of diffraction intensity, a higher-pressure data collection was not attempted. However, the pressure cell was loosened slightly and a second high-pressure data collection was made. Unit-cell parameters (Table 1)

TABLE 2. Olivine positional parameters and isotropic temperature factors

Atom	Parameter	HCP*	Fayalite: P=1 atm, -196°C	Fayalite: P=1 atm, In P-cell, 23°C	Fayalite: P=1 atm, 23°C	Fayalite: T = 23°C, <1 kbar	Fayalite: T = 23°C, 42 kbar	Fayalite: T = 23°C, 31 kbar	Hortonolite: P = 1 atm, 23°C	Hortonolite: P = 1 atm, 300°C	Hortonolite: P = 1 atm, 600°C	Hortonolite: P = 1 atm, 900°C
M(1)	X	0	0	0	0	0	0	0	0	0	0	0
	Y	0	0	0	0	0	0	0	0	0	0	0
	Z	0	0	0	0	0	0	0	0	0	0	0
	B		0.36(2)†	0.27(5)	0.48(2)	0.27(5)	0.8(2)	0.3(1)	0.44(2)	1.02(3)	1.52(3)	2.37(7)
	$\bar{\mu}'$		0.068	0.058	0.078	0.06	0.10	0.06	0.074	0.113	0.138	0.173
M(2)	X	0	0.9861(3)	0.985(1)	0.9851(5)	0.985(1)	0.978(2)	0.987(2)	0.9867(1)	0.9876(2)	0.9878(2)	0.994(8)
	Y	1/4	0.2799(1)	0.279(1)	0.2803(2)	0.279(1)	0.278(2)	0.284(1)	0.2792(1)	0.2797(1)	0.2802(1)	0.2799(2)
	Z	1/4	1/4	1/4	1/4	1/4	1/4	1/4	1/4	1/4	1/4	1/4
	B		0.36(2)	0.27(5)	0.37(3)	0.27(5)	0.5(2)	0.5(1)	0.33(2)	0.81(4)	1.23(3)	1.69(7)
	$\bar{\mu}$		0.068	0.058	0.069	0.06	0.08	0.08	0.065	0.095	0.124	0.148
Si	X	3/8	0.4313(4)	0.426(1)	0.4292(7)	0.426(1)	0.421(2)	0.428(2)	0.4287(2)	0.4284(3)	0.4289(3)	0.445(15)
	Y	0.0833	0.0971(2)	0.095(2)	0.0973(4)	0.095(2)	0.110(4)	0.092(3)	0.0957(1)	0.0957(1)	0.0958(1)	0.0959(5)
	Z	1/4	1/4	1/4	1/4	1/4	1/4	1/4	1/4	1/4	1/4	1/4
	B		0.37(4)	0.036(10)	0.35(5)	0.36(10)	0.4(3)	0.0(2)	0.33(1)	0.69(3)	0.96(3)	1.06(9)
	$\bar{\mu}$		0.069	0.068	0.067	0.07	0.07	0.0	0.065	0.094	0.110	0.115
O(1)	X	3/4	0.7684(11)	0.772(2)	0.7680(18)	0.772(2)	0.763(6)	0.771(5)	0.7661(5)	0.7649(8)	0.7632(7)	0.814(62)
	Y	0.0833	0.0905(6)	0.098(4)	0.0907(8)	0.098(4)	0.092(9)	0.107(6)	0.0918(2)	0.0921(4)	0.0926(3)	0.0882(14)
	Z	1/4	1/4	1/4	1/4	1/4	1/4	1/4	1/4	1/4	1/4	1/4
	B		0.51(11)	0.0(2)	0.36(13)	0.0(2)	0.5(7)	-0.8(5)	0.49(2)	0.98(3)	1.29(4)	2.64(6)
	$\bar{\mu}$		0.080	0.0	0.068	0.0	0.08	0.0	0.079	0.111	0.128	0.187
O(2)	X	1/4	0.2075(12)	0.216(2)	0.2079(18)	0.216(2)	0.225(7)	0.237(5)	0.2127(6)	0.2135(9)	0.2123(7)	0.210(12)
	Y	0.4167	0.4547(6)	0.450(4)	0.4551(8)	0.450(4)	0.474(11)	0.479(9)	0.4514(2)	0.4524(4)	0.4514(3)	0.4503(9)
	Z	1/4	1/4	1/4	1/4	1/4	1/4	1/4	1/4	1/4	1/4	1/4
	B		0.47(10)	-0.1(2)	0.33(13)	-0.1(2)	0.5(7)	-0.8(4)	0.50(2)	0.91(3)	1.37(3)	0.89(14)
	$\bar{\mu}$		0.077	0.0	0.065	0.0	0.08	0.0	0.80	0.107	0.131	0.100
O(3)	X	1/4	0.2875(8)	0.281(1)	0.2890(12)	0.281(1)	0.285(5)	0.314(3)	0.2844(4)	0.2847(6)	0.2853(5)	0.280(10)
	Y	0.1667	0.1646(4)	0.164(3)	0.1650(5)	0.164(3)	0.163(7)	0.159(4)	0.1633(2)	0.1631(2)	0.1631(2)	0.1615(6)
	Z	0	0.0359(7)	0.042(1)	0.0403(9)	0.042(1)	0.044(3)	0.040(2)	0.0357(3)	0.0375(5)	0.0370(4)	0.0447(12)
	B		0.52(7)	0.2(2)	0.58(10)	0.2(2)	1.4(5)	-0.3(4)	0.55(3)	1.04(4)	1.48(4)	1.84(14)
	$\bar{\mu}$		0.081	0.050	0.085	0.05	0.13	0.0	0.083	0.114	0.136	0.152

*"Ideal" hexagonal close-packed olivine model

†Parenthesized figures refer to the esd of least units cited.

TABLE 3. Olivine anisotropic temperature factor coefficients

Atom	ij of β_{ij}	fayalite		hortonolite		
		-196°C	23°C	23°C	300°C	600°C
M(1)	11	1.1(4)†	5.8(6)	3.1(2)	7.9(4)	12.4(4)
	22	0.9(1)	1.7(1)	1.5(1)	3.3(1)	4.9(1)
	33	4.7(3)	3.2(3)	2.8(1)	5.9(2)	8.4(2)
	12	0.1(2)	0.7(4)	0.1(1)	-0.0(2)	0.1(1)
	13	-0.2(3)	-1.3(6)	-0.7(2)	-1.1(3)	-1.8(3)
	23	-0.2(1)	-0.3(2)	0.5(1)	-1.2(1)	-1.7(1)
M(2)	11	1.8(4)	4.5(8)	3.8(2)	9.7(5)	15.6(4)
	22	0.8(1)	1.1(1)	0.7(1)	1.7(1)	2.4(1)
	33	4.6(3)	3.2(3)	2.4(1)	5.4(3)	8.0(2)
	12	0.0(2)	0.3(4)	0.1(1)	0.1(2)	0.2(1)
Si	11	1.2(7)	5.4(1.4)	1.9(3)	4.9(5)	7.5(5)
	22	0.8(2)	0.7(3)	1.0(1)	2.0(1)	2.6(1)
	33	6.1(5)	3.3(7)	2.8(2)	5.1(3)	7.0(3)
	12	0.5(3)	0.5(5)	0.0(1)	0.1(2)	0.3(2)
O(1)	11	0.4(1.9)	2.3(3.5)	2.6(9)	8.0(1.7)	8.9(1.5)
	22	1.4(5)	0.7(8)	1.7(2)	3.0(4)	4.1(3)
	33	8.9(1.5)	6.8(2.1)	3.2(5)	6.3(9)	8.5(8)
	12	1.0(8)	0.6(1.6)	0.1(4)	0.1(7)	0.3(6)
O(2)	11	1.6(2.0)	3.7(3.5)	6.8(1.0)	11.5(1.9)	18.4(1.6)
	22	1.3(5)	0.1(7)	0.7(2)	1.7(3)	1.9(3)
	33	8.6(1.5)	5.8(1.9)	3.9(5)	6.2(9)	10.4(9)
	12	0.7(8)	-1.2(1.3)	0.1(3)	-0.6(6)	-0.6(5)
O(3)	11	3.6(1.3)	5.3(2.1)	5.1(1)	8.8(1.0)	14.4(1.0)
	22	1.2(3)	1.5(5)	1.5(4)	3.2(2)	4.3(2)
	33	7.1(1.0)	6.3(1.5)	3.6(4)	6.3(7)	8.3(7)
	12	-0.2(5)	0.5(1.0)	0.6(2)	0.8(4)	1.4(4)
	13	1.1(1.1)	2.5(1.0)	0.2(4)	-0.1(8)	0.3(7)
	23	-0.3(5)	-0.4(7)	0.5(2)	0.9(4)	1.6(3)

*$\beta_{ij} \times 10^3$; for M(2), Si, O(1) and O(2) $\beta_{13} = \beta_{23} = 0$. P = 1 atm for all data.
†Parenthesized figures refer to the esd of least units cited.

suggested a pressure of approximately 31 ± 4 kbar. Only 286 of 979 collected reflections were observed, and refinement of these data converged at a weighted R = 5.6 percent (unweighted = 8.7%).

Results

Thermal expansion, bond distances, and bond angles

Linear and volume thermal expansion of several ferromagnesian olivines are plotted in Figures 1 and 2. All four olivines graphed, from forsterite to fayalite, have approximately parallel expansion curves for cell edges and volumes from −196° to 1000°C. Thus Mg/Fe ratio appears to have little effect on the bulk and linear thermal expansivities of ferromagnesian olivines.

Fayalite and hortonolite bond distances and angles are given in Tables 4 and 5. Silicon–oxygen bond distances show no change within experimental error with temperature or pressure, whereas $(Fe,Mg)O_6$ octahedra show significant expansion and compression. Because of limited amount and quality of high-pressure data, detailed analysis of individual bonds and angles of the high-pressure refinements has not proved profitable.

Hazen (1976a) noted that expansion rates of individual Mg–O bonds in forsterite varied, with the shortest bonds expanding at $\approx 2 \times 10^{-5}$ A/K versus 5×10^{-5} A/K for the longest bonds. However, fayalite Fe–O octahedral distances show little variation in expansion; all Fe–O bonds expand at $\approx 3 \times 10^{-5}$ A/K except for the two shortest $M(2)$–O bonds [$M(2)$–O(2) and $M(2)$–O(3″) expand at ≈4 and 0.5×10^{-5} A/K respectively]. This difference in Mg–O and

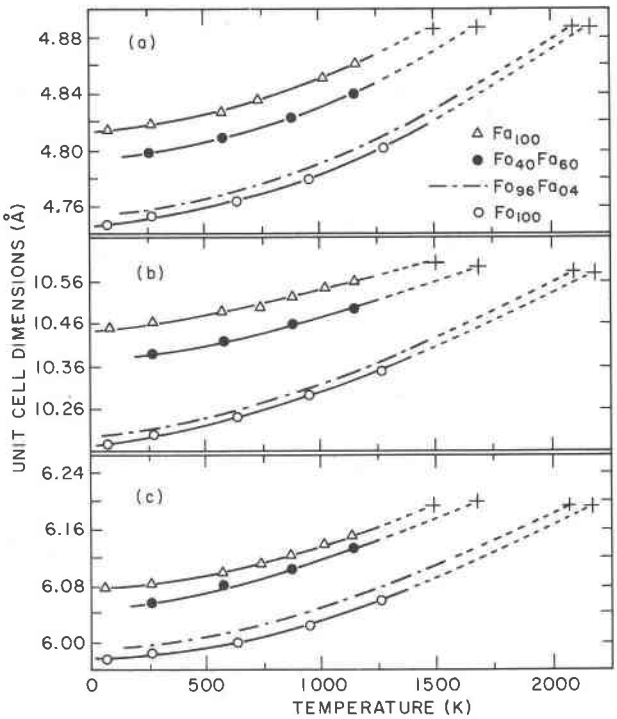

FIG. 1. Olivine unit-cell dimensions versus temperature. Fa_{100} data from Smyth (1975), $Fo_{96}Fa_{04}$ data from Skinner (1962), Fo_{100} data from Hazen (1976a). Dashed portions of lines represent extrapolations from known data to the melting point, assuming a quadratic equation in T for linear thermal expansions.

Fe–O expansion behavior in olivines may be the result of greater covalency of the iron–oxygen bond.

Temperature factors

Anisotropic temperature factors and corresponding magnitudes and orientations of thermal ellipsoids for fayalite and hortonolite at several temperatures appear in Tables 3 and 6 respectively. No major changes in cation vibration orientation is observed with changing composition or with temperature. Anisotropic temperature factors have not been calculated for the pressure-cell fayalite data refinements.

Coordination polyhedral volumes and polyhedral distortions

Polyhedral volumes for $M(1)$, $M(2)$, and Si have been calculated from fayalite structural data for conditions from −196° to 900°C (including data of Smyth, 1975), and for hortonolite polyhedra at 23°, 300°, and 600°C, and these volumes are given in Table 7. As in forsterite (Hazen, 1976a) and a previous refinement of hortonolite (Fo_{69} Fa_{31}) by Brown and Prewitt (1973), both ferro-olivine octahedra show significant thermal expansion, whereas there is little change in Si tetrahedral volume over the temperature interval studied.

From −196° to 900°C the net change in fayalite unit-cell volume is 10 A³. Contributing to this volume increase are 0.4 A³ from each $M(1)$ and 0.5 A³ from each $M(2)$, giving a net polyhedral volume increase of 3.6A³. Thus more than 60% of fayalite's thermal expansion is due to the expansion of unoccupied octahedral and tetrahedral sites in the close-packed array. Similar behavior is observed for forsterite and intermediate Fe–Mg olivines.

Bond-angle strain, bond-angle variance, and mean polyhedral quadratic elongation (as defined by Robinson *et al.*, 1971) for fayalite and hortonolite at several temperatures are given in Table 7. Bond-angle strains and bond-angle variances for both $M(1)$ and $M(2)$ octahedra increase with temperature, and are greater for higher iron content. However, SiO_4 distortions decrease slightly with increasing temperature, as well as with increasing iron content. For all three olivines considered, octahedral bond-angle strains and variances have significantly greater distortion indices than do SiO_4 tetrahedra. These observations are consistent with previous polyhedral dis-

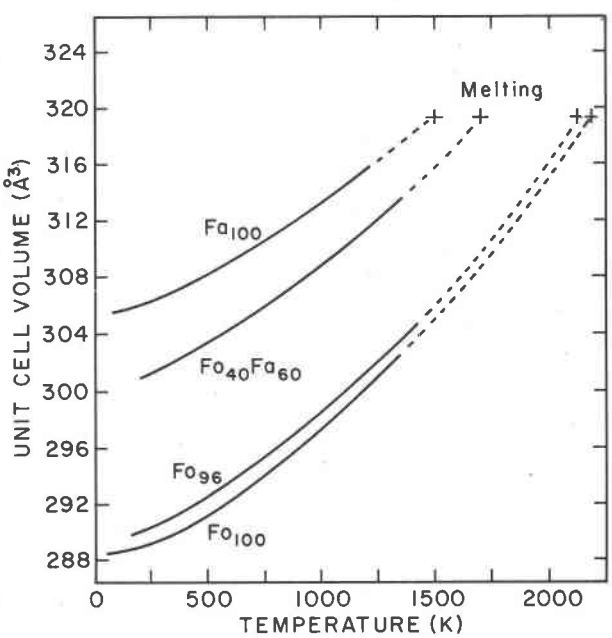

FIG. 2. Olivine unit-cell volume versus temperature. Volumes are calculated from linear expansion data recorded in Fig. 1.

TABLE 4. Olivine bond distances

Bond	[Multiplicity]	Fayalite: P = 1 atm -196°C	Fayalite: P = 1 atm 23°C	Fayalite: T = 23°C P < 1 kbar	Fayalite: T = 23°C 42 kbar	Fayalite: T = 23°C 31 kbar	Hortonolite: P = 1 atm 23°C†	Hortonolite: P = 1 atm 300°C†	Hortonolite: P = 1 atm 600°C†	Hortonolite: P = 1 atm 900°C†
Si Tetrahedron										
Si-O(1)	[1]	1.624(6)[d]	1.634(10)	1.67(1)	1.56(12)	1.55(12)	1.619(3)	1.619(3)	1.612(3)	1.60(3)
Si-O(2)	[1]	1.630(6)	1.630(9)	1.66(4)	1.65(14)	1.40(14)	1.646(3)	1.642(3)	1.644(3)	1.68(4)
Si-O(3)	[2]	1.634(4)	1.609(6)	1.62(2)	1.50(10)	1.65(10)	1.630(3)	1.625(3)	1.632(3)	1.58(5)
mean Si-O		1.631	1.621	1.64	1.55	1.56	1.629	1.626	1.633	1.638
O(1)-O(2)	[1]	2.695(8)	2.697(12)	2.82(3)	2.64(9)	2.70(11)	2.724(4)	2.723(6)	2.720(5)	2.0(2)
O(1)-O(3)	[2]	2.766(7)	2.750(10)	2.77(2)	2.71(7)	2.59(9)	2.753(4)	2.748(5)	2.747(4)	2.1(2)
O(2)-O(3)‡	[2]	2.549(6)	2.542(9)	2.57(4)	2.3(2)	2.3(2)	2.555(3)	2.548(5)	2.554(4)	2.55(1)
O(3)-O(3)‡	[1]	2.602(8)	2.553(12)	2.54(2)	2.5(2)	2.55(19)	2.595(5)	2.584(6)	2.599(6)	2.53(2)
mean O-O		2.655	2.639	2.67	2.53	2.49	2.656	2.649	2.651	2.3
M(1) Octahedron										
M(1)-O(1)	[2]	2.108(4)	2.113(6)	2.14(2)	2.11(9)	2.17(9)	2.112(2)	2.124(3)	2.138(3)	2.21(4)
M(1)-O(2)	[2]	2.125(4)	2.125(6)	2.11(1)	2.02(11)	1.99(12)	2.106(2)	2.111(3)	2.120(3)	2.16(4)
M(1)-O(3)	[2]	2.218(4)	2.233(6)	2.20(2)	2.17(10)	2.24(13)	2.188(2)	2.194(3)	2.203(3)	2.21(4)
mean M(1)-O		2.150	2.157	2.15	2.10	2.13	2.135	2.143	2.154	2.192
O(1)-O(3)‖	[2]	2.921(7)	2.922(10)	2.84(1)	2.89(4)	2.9(1)	2.902(4)	2.909(5)	2.928(4)	3.3(3)
O(1)-O(3')	[2]	3.193(6)	3.220(10)	3.28(5)	3.17(7)	3.27(7)	3.174(3)	3.191(5)	3.205(4)	3.17(3)
O(1)-O(2)‖	[2]	2.894(8)	2.897(12)	2.91(3)	2.74(14)	2.77(12)	2.892(4)	2.900(6)	2.922(5)	2.95(7)
O(1)-O(2')	[2]	3.089(2)	3.094(4)	3.097(9)	3.10(10)	3.17(19)	3.071(3)	3.085(3)	3.097(3)	3.13(4)
O(2)-O(3')	[2]	3.517(3)	3.541(5)	3.46(2)	3.52(11)	3.54(13)	3.453(4)	3.471(5)	3.488(5)	3.54(7)
O(2)-O(3)‡	[2]	2.549(6)	2.542(9)	2.57(4)	2.3(2)	2.26(12)	2.555(3)	2.548(5)	2.554(4)	2.55(1)
mean O-O		3.027	3.036	3.03	2.95	2.99	3.008	3.017	3.032	3.11
M(2) Octahedron										
M(2)-O(1)	[1]	2.238(6)	2.244(9)	2.15(4)	2.17(5)	2.09(6)	2.216(2)	2.229(4)	2.241(4)	2.6(2)
M(2)-O(2)	[1]	2.115(6)	2.122(9)	2.11(3)	2.33(7)	2.34(9)	2.094(2)	2.102(4)	2.104(4)	2.05(4)
M(2)-O(3)	[2]	2.066(4)	2.084(6)	2.11(1)	2.09(11)	2.39(15)	2.275(2)	2.277(3)	2.291(3)	2.24(5)
M(2)-O(3")	[2]	2.291(4)	2.287(6)	2.26(2)	2.26(5)	2.03(7)	2.071(2)	2.089(3)	2.091(3)	2.17(4)
mean M(2)-O		2.178	2.184	2.13	2.28	2.31	2.167	2.177	2.184	2.25
O(1)-O(3")	[2]	3.094(6)	3.111(10)	3.06(5)	3.07(6)	3.0(1)	3.077(3)	3.094(5)	3.099(4)	3.17(3)
O(1)-O(3)‖	[2]	2.921(7)	2.922(10)	2.84(1)	2.89(4)	2.9(1)	2.902(4)	2.909(5)	2.928(4)	3.3(3)
O(2)-O(3)	[2]	3.321(5)	3.317(6)	3.33(4)	3.43(8)	3.5(2)	3.280(4)	3.297(5)	3.315(5)	3.31(2)
O(2)-O(3'")	[2]	2.943(6)	2.963(9)	3.00(2)	3.1(1)	2.98(7)	2.941(3)	2.959(5)	2.962(4)	2.97(6)
O(3)-O(3)‡	[1]	2.602(8)	2.553(12)	2.54(2)	2.5(1)	2.55(5)	2.595(5)	2.584(6)	2.599(6)	2.53(2)
O(3)-O(3")	[2]	3.028(5)	3.035(7)	3.05(4)	3.04(4)	3.08(5)	3.031(3)	3.044(4)	3.054(4)	3.07(1)
O(3")-O(3'")	[1]	3.474(2)	3.533(2)	3.527(6)	3.56(3)	3.52(7)	3.460(5)	3.496(7)	3.502(6)	3.59(2)
mean O-O		3.091	3.065	3.052	3.09	3.08	3.043	3.057	3.068	3.15

*All distances in Å.
†Data of Smyth and Hazen (1973), revised.
‡Edge shared between an octahedron and tetrahedron.
§Parenthesized figures refer to the esd of least figures cited.
‖Edge shared between two octahedra.

tortion calculations for olivines by Birle *et al.* (1968), Brown (1970), and Brown and Prewitt (1973).

Discussion

Crystal melting—a structurally controlled phenomenon?

Melting phenomena have traditionally been discussed in terms of thermodynamic equilibrium (*e.g.* Broecker and Oversby, 1971, Chapter 10), and predictions of melting are usually based on thermodynamic calculations (*e.g.* Bradley, 1962). Less emphasis has been placed in the mineralogical literature on the structural origins of melting (however, see Ubbelohde, 1965). While any treatment of crystal melting must account for properties of both solid and liquid phases, it is intuitively interesting to examine crystal structures near their melting points for structural weaknesses which might facilitate breakdown to a melt.

Data of the present study allows extrapolation of ferromagnesian olivine structures to their melting points. Unit-cell edges are plotted versus temperature in Figure 1, and are extrapolated to melting for forsterite, two intermediate olivines, and fayalite. Extrapolations are based on least-squares fit of cell-edge thermal expansion data to a quadratic equation. All olivines plotted have similar cell constants of a =

TABLE 5. Olivine bond angles

		Fayalite: P = 1 atm		Fayalite: T = 23°C			Hortonolite: P = 1 atm			
Angle	[Multiplicity]	-196°C	23°C	P<1 kbar	42 kbar	31 kbar	23°C†	300°C†	600°C†	900°C†
O(1)-Si-O(2)	[1]	111.8(3)*	111.5(5)	115(1)	114(2)	116(2)	113.1(2)	113.2(2)	113.3(2)	113(3)
O(1)-Si-O(3)	[2]	116.2(3)	116.0(3)	116(2)	110(4)	114(4)	115.8(1)	115.8(1)	115.7(1)	116(3)
O(2)-Si-O(3)	[2]	102.7(2)	103.5(3)	103(2)	97(5)	100(4)	102.5(1)	102.5(2)	102.5(1)	103(3)
O(3)-Si-O(3')	[1]	105.5(3)	105.0(4)	103(1)	114(7)	110(6)	105.5(1)	105.3(2)	105.6(2)	107(5)
mean O-Si-O		109.2	109.3	109	107	112	108.9	109.2	109.2	111
O(1)-M(1)-O(3)	[2]	84.9(2)	84.4(3)	81.8(9)	85(3)	81(3)	84.9(1)	84.7(1)	84.8(1)	81(3)
O(1)-M(1)-O(3')	[2]	95.1(2)	95.6(3)	98.2(9)	95(4)	99(4)	95.1(1)	95.3(1)	95.2(1)	99(3)
O(1)-M(1)-O(2)	[2]	86.3(2)	86.2(2)	86.5(7)	83(4)	84(3)	86.6(1)	86.5(1)	86.7(1)	81(3)
O(1)-M(1)-O(2')	[2]	93.7(2)	93.8(2)	93.5(7)	97(4)	96(4)	93.4(1)	93.5(1)	93.3(1)	99(3)
O(2)-M(1)-O(3')	[2]	108.1(2)	108.7(3)	107(11)	113(5)	115(5)	107.0(1)	107.4(1)	107.6(1)	109(1)
O(2)-M(1)-O(3)	[2]	71.9(3)	71.3(3)	73(11)	67(4)	65(5)	73.0(1)	72.6(1)	72.4(1)	71(1)
mean O-M(1)-O		90	90	90	90	90	90	90	90	90
O(1)-M(2)-O(3")	[2]	91.8(3)	91.8(2)	91.6(9)	92(1)	93(2)	91.7(1)	91.5(1)	91.3(1)	91(2)
O(1)-M(2)-O(3)	[2]	80.3(2)	80.3(3)	80.2(9)	81(2)	81(3)	80.5(1)	80.4(1)	80.5(1)	83(3)
O(2)-M(2)-O(3)	[2]	97.8(2)	97.6(3)	96.9(8)	97(3)	97(3)	97.2(1)	97.6(1)	97.8(1)	100(2)
O(2)-M(2)-O(3"')	[2]	89.5(1)	89.6(2)	90.4(8)	89(1)	88(2)	89.9(1)	89.8(1)	89.8(1)	89(1)
O(3)-M(2)-O(3')	[1]	69.2(2)	67.9(2)	68.4(7)	67(3)	64(3)	69.6(1)	69.1(2)	69.1(1)	68(2)
O(3)-M(2)-O(3")	[2]	87.9(1)	87.8(2)	88.5(7)	88(1)	88(1)	88.3(1)	88.3(1)	88.2(1)	89(1)
O(3)-M(2)-O(3"')	[1]	114.4(2)	116.0(3)	114.1(8)	116(4)	120(5)	113.3(1)	113.6(2)	113.7(1)	114(3)
mean O-M(2)-O		89.9	89.8	89.8	92.3	89.9	89.8	89.8	89.8	90.5

*Parenthesized figures refer to the esd of least units cited.

†Data of Smyth and Hazen (1973), revised.

4.89, $b = 10.6$, and $c = 6.19$ A at melting, resulting in a cell volume of 319 A^3 (Fig. 2). Other olivine structural parameters may be extrapolated in a similar way. For example, fayalite at melting has mean $M(1)$– and $M(2)$–O bond distances of 2.19 and 2.22 A. In these and other structure parameters the melting-point projected values of the different olivines are similar; it thus appears that the ferromagnesian olivine solidus represents an isostructural line. It seems possible that the melting of olivine is in part structurally controlled, perhaps due to misfit of expanding octahedra with rigid tetrahedra, and that the "solidus structure" represents a critical structural limit for the ferromagnesian olivines.

The existence of a solidus/liquidus melting relationship is easily explained using this model. An intermediate olivine is heated and expands up to a limiting structure at which the octahedra are at their maximum possible size with respect to the rigid SiO_4 tetrahedra. As the temperature is raised further, an iron-rich liquid is "expelled" to reduce the effective octahedral volume and maintain the limiting structure.

The olivine/spinel transformation

High-pressure solid-phase equilibria require the characterization of two crystalline solids, and geometrical constraints of both structures must be considered. Olivine and spinel are both closed-packed oxides with 6-coordinated (Mg,Fe) and 4-coordinated Si. Kamb (1968) noted that a significant difference in polyhedral packing of these two structures is the number and type of shared edges; the greater number of shared edges in spinel allows the close approach of more octahedral cations in that structure. Thus spinel is the denser of the two forms. Kamb used the ratio of mean octahedral metal–oxygen bond length (d_B) to mean tetrahedral bond length (d_A) to predict the relative stabilities of olivine versus spinel polymorphs. In general, for compounds of the form $B_2^{2+}AO_4$, if $(d_B)/(d_A) > 1.19$ then the olivine structure is stable, whereas if $(d_B)/(d_A) < 1.19$ then spinel is the stable form.[2] Forsterite and fayalite at room T and P have ratios of 1.30 and 1.33 respectively, suggesting that the olivine structure should indeed be stable. However, as pressure is increased, the octahedra compress while tetrahedra remain unchanged. In this way $(d_B)/(d_A)$ is lowered, and eventually a transition to the spinel form will occur.

[2] In fact, the critical ratio of 1.19 may vary depending on A. In silicates Kamb's data suggests that a slightly higher value of 1.21 is perhaps more realistic.

Mantle olivine structure—a prediction

Conditions in the upper mantle at a depth of 100 km have been projected to be approximately 1000°C and 30 kbar, and olivine compositions of approximately $Fo_{90}Fa_{10}$ are suggested by known Mg/Fe ratios in mantle-derived nodules (Wyllie, 1971). Between 23° and 1000°C, forsterite expands by 3.8 percent. At 1000°C, forsterite's bulk modulus is approximately 1190 kbar ($K_{23°}$ = 1350 kbar, Hazen, 1976a; dK/dT = 0.16 kbar/°C, Graham and Barsch, 1969). A 30 kbar increase in pressure at 1000°C will cause an approximate 2.5 percent decrease in volume. Thus, the net volume change is approximately +1.3

TABLE 6. Magnitudes and orientations of olivine thermal ellipsoids*

		M(1)				M(2)				SI			
T(°C)	i of r_i	r_i	a	b	c	r_i	a	b	c	r_i	a	b	c
Fayalite													
	1	0.0351(6)†	6(5)	95(6)	88(4)	0.046(5)	2(10)	92(10)	90	0.031(14)	19(10)	109(10)	90
-196	2	0.071(3)	94(6)	169(6)	100(6)	0.068(3)	92(10)	178(10)	90	0.069(7)	109(10)	161(10)	90
	3	0.094(3)	93(4)	100(5)	10(6)	0.093(3)	90	90	0	0.106(5)	90	90	0
	1	0.067(7)	48(11)	95(14)	42(13)	0.070(8)	31(29)	121(20)	90	0.057(13)	67(20)	157(20)	90
23	2	0.082(7)	57(15)	129(9)	124(16)	0.078(4)	90	90	180	0.079(8)	90	90	180
	3	0.104(6)	121(8)	141(9)	68(8)	0.080(7)	59(29)	31(29)	90	0.083(10)	23(20)	67(20)	90
Hortonolite													
	1	0.056(2)	29(5)	84(3)	62(5)	0.060(2)	73(13)	163(13)	90	0.047(4)	1(5)	91(5)	90
23	2	0.071(2)	62(5)	114(3)	141(5)	0.066(2)	90	90	180	0.072(3)	90	90	180
	3	0.093(1)	97(3)	155(3)	66(3)	0.067(2)	17(13)	73(13)	90	0.073(2)	89(5)	1(5)	90
	1	0.088(3)	44(6)	77(3)	49(5)	0.096(2)	81(11)	171(11)	90	0.075(4)	3(6)	93(6)	90
300	2	0.104(3)	47(6)	109(3)	131(5)	0.100(2)	90	90	180	0.098(3)	90	90	180
	3	0.141(2)	94(2)	157(2)	67(2)	0.107(3)	9(11)	81(11)	90	0.105(3)	87(6)	3(6)	90
	1	0.107(2)	51(3)	75(2)	43(3)	0.115(2)	86(4)	176(4)	90	0.094(3)	7(5)	97(5)	90
600	2	0.129(2)	40(3)	108(2)	124(3)	0.123(2)	90	90	180	0.115(2)	90	90	180
	3	0.172(1)	95(2)	156(1)	67(1)	0.136(2)	4(4)	86(4)	90	0.120(2)	83(5)	7(5)	90

		O(1)				O(2)				O(3)			
T(°C)	i of r_i	r_i	a	b	c	r_i	a	b	c	r_i	a	b	c
Fayalite													
	1	0.06(1)	34(10)	124(10)	90	0.04(3)	17(18)	107(18)	90	0.06(1)	169(16)	97(30)	81(11)
-196	2	0.09(1)	124(10)	146(10)	90	0.09(1)	107(18)	163(18)	90	0.08(1)	85(30)	169(21)	100(13)
	3	0.11(1)	90	90	0	0.13(1)	90	90	0	0.12(1)	80(9)	99(12)	13(11)
	1	0.04(6)	32(61)	122(61)	90	0.03(4)	12(37)	102(37)	90	0.06(2)	146(18)	71(25)	64(13)
23	2	0.07(3)	122(61)	148(61)	90	0.08(3)	102(37)	168(37)	90	0.10(2)	69(25)	21(25)	92(29)
	3	0.11(2)	90	90	0	0.08(2)	90	90	0	0.12(1)	65(15)	98(29)	26(13)
Hortonolite													
	1	0.055(9)	3(8)	93(8)	90	0.061(8)	88(12)	178(12)	90	0.070(5)	47(24)	125(8)	63(24)
23	2	0.077(6)	90	90	180	0.085(6)	90	90	180	0.077(5)	51(25)	81(17)	139(20)
	3	0.098(5)	87(8)	3(8)	90	0.089(6)	2(12)	88(12)	90	0.099(4)	69(8)	36(7)	62(8)
	1	0.097(11)	2(15)	92(15)	90	0.094(10)	72(18)	18(18)	90	0.096(7)	36(28)	112(9)	63(27)
300	2	0.109(8)	90	90	180	0.108(8)	90	90	180	0.106(7)	57(29)	79(13)	145(24)
	3	0.127(8)	88(15)	2(15)	90	0.118(9)	18(18)	108(18)	90	0.138(5)	78(7)	25(7)	69(8)
	1	0.102(9)	4(8)	94(8)	90	0.102(8)	83(7)	7(7)	90	0.112(6)	73(14)	119(4)	35(11)
600	2	0.126(6)	90	90	180	0.140(6)	90	90	180	0.128(5)	25(11)	97(9)	114(13)
	3	0.150(6)	86(8)	4(8)	90	0.148(6)	7(7)	97(7)	90	0.166(4)	72(5)	31(4)	66(4)

*P = 1 atm for all data.

†Parenthesized figures refer to the esd of least units cited.

TABLE 7. Olivine polyhedral volumes and distortions

Site	Parameter	Fayalite -196°C	Fayalite 23°C	Fayalite 20°C	Fayalite 300°C	Fayalite 600°C	Fayalite 900°C	Hortonolite 23°C	Hortonolite 300°C	Hortonolite 600°C
M(1)	Octahedral Volume (Å^3)	12.89	12.93	12.92	12.99	13.12	13.22	12.69	12.75	12.92
	Ideal Volume (Å^3)	13.25	14.00	13.38	13.47	13.62	13.83	12.98	13.12	13.33
	Bond Angle Strain	36.2	37.4	36.2	36.6	36.8	38.2	34.0	34.8	35.2
	Angle Variance	133.6	143.8	135.6	137.6	139.5	150.8	118.8	124.8	126.4
	Quadratic Elongation	1.042	1.047	1.039	1.037	1.035	1.038	1.033	1.032	1.030
M(2)	Octahedral Volume (Å^3)	13.47	13.56	13.37	13.54	13.80	13.97	13.23	13.42	13.41
	Ideal Volume (Å^3)	13.78	13.89	13.80	13.95	14.12	14.35	13.57	13.76	13.89
	Bond Angle Strain	45.0	48.1	46.9	47.7	48.1	50.1	43.7	44.5	44.6
	Angle Variance	123.1	135.0	129.0	132.2	134.0	144.9	114.1	115.6	115.8
	Quadratic Elongation	1.090	1.082	1.088	1.088	1.087	1.078	1.085	1.080	1.086
Si	Tetrahedral Volume (Å^3)	2.22	2.17	2.19	2.18	2.19	2.15	2.21	2.19	2.20
	Ideal Volume (Å^3)	2.23	2.19	2.21	2.20	2.21	2.19	2.22	2.21	2.23
	Bond Angle Strain	13.5	12.5	12.6	12.7	12.5	12.0	13.3	13.3	13.2
	Angle Variance	34.1	25.4	26.6	26.3	25.6	24.3	29.3	30.3	29.3
	Quadratic Elongation	1.004	1.014	1.020	1.025	1.028	1.041	1.009	1.008	1.010

percent. In particular, an olivine of composition $Fo_{90}Fa_{10}$ with room-temperature lattice parameters of $a = 4.76$, $b = 10.21$, $c = 5.99$ A, and volume = 291 A^3, would have approximate unit-cell dimensions of $a = 4.775$, $b = 10.27$, $c = 6.02$ A and volume of 295 A^3 at 1000°C and 30 kbar. These lattice constants are almost identical to those of a pure forsterite at about 600°C and 1 atm, as described in Hazen (1976a). If the assumption is made that the SiO_4 tetrahedron does not change size or shape, and with the observation that occupied octahedral sites and voids compress or expand at approximately the same rate, the structure of 100 km mantle olivine may be projected to be similar to that of 600°C forsterite. While structural details undoubtedly differ to some extent, the basic size and shape of these two olivines, and in fact any two ferromagnesian olivines with the same unit-cell volumes, are predicted to be similar. It is generally accepted that mantle mineral assemblages are significantly denser than crustal rocks. It is therefore interesting that mantle olivine is projected to be less dense than olivine at room temperature and pressure.

Ferromagnesian olivine equation of state

The above prediction of mantle olivine's structure at 100 km illustrates the method of calculation of a structure at any given P, T, and Mg/Fe ratio. At room temperature and pressure, the unit-cell volume is $V = 290 + 17X_{Fe}$ A^3, where X_{Fe} is the mole fraction of octahedral Fe (from Fig. 2). The effect of temperature on unit-cell volume is approximately $\Delta V = 0.006T + 0.000006T^2$ A^3, where T is in °C (calculated

from data in Fig. 2). The bulk modulus of ferromagnesian olivines is approximately $K = 1350$ kbar (see *e.g.* Hazen, 1976a) and $dK/dT = 0.16$ kbar/°C; thus the effect of pressure on ferromagnesian unit-cell volume is given by:

$$-\Delta V = (V_{x,T} \cdot P)/(1350 - 0.16T)\ \text{A}^3,$$

where P is in kbar and T is in °C. Combining the several expressions above, the equation of state for ferro-magnesian olivine is predicted to be:

$$V = (290 + 17X_{\text{Fe}} + 0.006T + 0.000006T^2)\{1 - [P/(1350 - 0.16T)]\}\ \text{A}_3.$$

It has been assumed that $\delta\alpha/\delta X$, dK/X, and $\delta K/\delta P$ are approximately zero. Since olivine volume changes correspond to structural changes in a regular way, the equation of state also defines the structure of ferromagnesian olivines as a function of temperature, pressure, and composition.

Acknowledgments

The author gratefully acknowledges the advice and encouragement of Professor Charles W. Burnham. The manuscript was greatly improved by the thoughtful and thorough reviews of Professors Gordon Brown and Charles T. Prewitt. Thanks are also due to Professor R. G. Burns, Dr. T. L. Grove, Professor J. F. Hays, and Professor T. Shankland for their helpful discussions of the ideas in this study. This research was supported by National Science Foundation grants GA-12852 and GA-41415 (to C. W. Burnham, Harvard University).

References

Adams, L. H. (1931) The compressibility of fayalite, and the velocity of elastic waves in peridotite with different iron–magnesium ratios. *Beitr. Geophys., 31,* 315–321.

Birle, J. D., G. V. Gibbs, P. B. Moore and J. V. Smith (1968) Crystal structures of natural olivines. *Am. Mineral., 53,* 807–824.

Bradley, R. S. (1962) Thermodynamic calculations on phase equilibria involving fused salts. Part II. Solid solutions and applications to the olivines. *Am. J. Sci., 260,* 550–554.

Broecker, W. S. and V. M. Oversby (1971) *Chemical Equilibria in the Earth.* McGraw-Hill, New York, 318 p.

Brown, G. E. (1970) *Crystal chemistry of the olivines.* Ph.D. Thesis, Virginia Polytechnic Institute, Blacksburg, Virginia.

——— and C. T. Prewitt (1973) High-temperature crystal chemistry of hortonolite. *Am. Mineral., 58,* 577–587.

Graham, E. and G. Barsch (1969) Elastic constants of single crystal forsterite as a function of temperature and pressure. *J. Geophys. Res., 74,* 5949–5960.

Hazen, R. M. (1976a) Effects of temperature and pressure on the crystal structure of forsterite. *Am. Mineral., 61, 1280–1293.*

——— (1976b) Effects of temperature and pressure on the cell dimension and X-ray temperature factors of periclase. *Am. Mineral., 61,* 266–271.

———and C. W. Burnham (1974) The crystal structures of gillespite I and II: a crystal structure at high pressure. *Am Mineral., 59,* 1166–1176.

——— and ——— (1975) Correction and addenda to the crystal structures of gillespite I and II. *Am. Mineral., 60,* 937–938.

Heinriques, A. (1957) The effect of cations on the optical properties and cell dimensions of knebelite and olivine. *Ark. Mineral. Geol., 2,* 305–313.

Kamb, B. (1968) Structural basis of the olivine–spinel relation. *Am. Mineral., 53,* 1439–1455.

Olinger, B. and P. M. Halleck (1974) Redetermination of the relative compressions of the cell edges of olivine. *J. Geophys. Res., 79,* 5535–5538.

Robinson, K., G. V. Gibbs and P. H. Ribbe (1971) Quadratic elongation: a quantitative measure of distortion in coordination polyhedra. *Science, 172,* 567–570.

Skinner, B. J. (1962) Thermal expansion of ten minerals. *U. S. Geol. Surv. Prof. Pap. 450D,* D109–D112.

Smyth, J. R. (1975) High temperature crystal chemistry of fayalite. *Am. Mineral., 60,* 1092–1097.

——— and R. M. Hazen (1973) The crystal structures of forsterite and hortonolite at several temperatures up to 900°C. *Am. Mineral., 58,* 588–593.

——— and T. M. Usselman (1974) The crystal structure of synthetic fayalite to 900°C. *EOS, 56,* 1201.

Ubbelohde, A. R. (1965) *Melting and Crystal Structure.* Clarendon Press, Oxford, 325 p.

Wyllie, P. J. (1971) *The Dynamic Earth: Textbook in Geoscience.* John Wiley and Sons, Inc., New York, 416 p.

Manuscript received, April 21, 1976; accepted for publication, September 30, 1976.